J. Amer. Soc. Hort. Sci. 149(1):50–60. 2024. https://doi.org/10.21273/JASHS05334-23

# Identification of Novel Quantitative Trait Loci Associated with Table Grape Fruit Quality Characteristics in a Segregating Population and Transferability of Existing Quality Markers

**Laise de Sousa Moreira and Matthew D. Clark**
*Department of Horticultural Science, University of Minnesota, Saint Paul, MN 55108, USA*

**Amy Tabb**
*US Department of Agriculture, Agricultural Research Service, Innovative Fruit Production, Improvement and Protection Unit, Kearneysville, WV 25430, USA*

**Avi Karn and Jason P. Londo**
*School of Integrative Plant Science, Cornell University, Geneva, NY 14456, USA*

**Cheng Zou and Qi Sun**
*Bioinformatics Facility, Cornell University, Ithaca, NY 14850, USA*

**Sonet van Zyl**
*California State University Fresno, Fresno, CA 93740, USA*

**Bernard Prins**
*US Department of Agriculture, Agricultural Research Service, National Clonal Germplasm Repository, Davis, CA 95616, USA*

**Jeff D. DeLong, Alanna Burhans, Hui-Ching Yang, and Rachel P. Naegele**
*US Department of Agriculture, Agricultural Research Service, San Joaquin Valley Agricultural Sciences Center, Parlier, CA 93648, USA*

**Keywords.** berry shape, berry size, berry weight, quantitative trait locus, *Vitis*

**Abstract. Grape (*Vitis*) production and fruit quality traits such as cluster size, berry shape, and timing of fruit development are key aspects when selecting cultivars for commercial production. Molecular markers for some, but not all, of these traits have been identified using biparental or association mapping populations. Previously identified markers were tested for transferability using a small (24 individual) test panel of commercially available grape cultivars. Markers had little to no ability to differentiate grape phenotypes based on the expected characteristics, except the marker for seedlessness. Using a biparental interspecific cross, 43 quantitative trait loci (QTLs) (previously identified and new genomic regions) associated with berry shape, number, size, cluster weight, cluster length, time to flower, veraison, and full color were detected. Kompetitive allele-specific polymerase chain reaction markers designed on newly identified QTLs were tested for transferability using the same panel. Transferability was low when use types were combined, but they were varied when use types were evaluated separately. A comparison of a 4-Mb region at the end of chromosome 18 revealed structural differences among grape species and use types. Table grape cultivars had the highest similarity in structure for this region (>75%) compared with other grape species and commodity types.**

Grapes, *Vitis* sp., are a high-value specialty crop grown worldwide. Global grape production in 2018 was valued at $167.9 billion when including table, raisin, and wine grapes and related products (juice, grape seed oil, grape leaves, others). Despite the high value, profit margins continue to decrease as expenses related to labor, chemical costs, and climate-related challenges increase (Fidelibus et al. 2018; Mira de Orduna 2010; Santos et al. 2020; van Leeuwen and Darriet 2016). These costs are in addition to regular recurring seasonal expenses such as the 10 to 14 standard pesticide applications needed to control diseases, and the sizing and coloring plant growth regulator sprays used in the California table grape industry to achieve uniformity. Breeding new grape cultivars with improved traits, such as early ripening and naturally large berry size, is one way to offset increasing production costs and broaden market access.

Although most cultivated table, raisin, and wine grapes are the same species (*Vitis vinifera*), the use type has dictated specific traits for each that can vary by region. Regarding table grapes, producers prefer cultivars with large, loose clusters and large berries. Wine grape producers prefer medium-size clusters with small, seeded berries for a higher skin-to-flesh ratio to enhance wine quality. Early breeding efforts for grapes focused on hermaphroditism, titratable acid-to-sugar ratios, yield, color, and seedlessness (table and raisin grapes only) (Burger et al. 2014; Myles et al. 2010; Terral et al. 2010; Yamada and Sato 2016). As breeding programs have advanced, additional traits have been added, such as disease resistance (e.g., grape powdery mildew caused by *Erysiphe necator*, Pierce's disease caused by *Xylella fastidiosa*, and others), ripening time, and increased cluster

size and weight. Selecting for the multiple traits needed for a single cultivar without tightly linked or predictive molecular markers is resource-demanding. Breeding for traits such as berry size and shape that historically have been managed by cultural or chemical practices (e.g., gibberellin sprays and girdling) can help to reduce labor and chemical costs, and selecting cultivars with earlier or later ripening times can expand the production window for a region while providing access to new national or international markets. However, to improve the selection efficiency of improved cultivars, additional transferable molecular tools are needed.

Previous studies have found quantitative trait loci (QTLs) associated with flowering and veraison time, berry size, and other fruit quality traits. Unfortunately, many of these traits are associated with multiple small-effect QTLs dispersed across the grape genome. Flowering time and veraison time were associated with the QTLs of varying effects on chromosomes 1, 4, 8, 9, 10, 11, 13, 14, 17, 18, and 19, depending on the parentage of the cross (Fechter et al. 2014; Kamal et al. 2019; Underhill et al. 2020). Two of those QTLs on chromosomes 1 and 17 were consistently identified in two populations evaluated across two years (Fechter et al. 2014). More recently, a genome-wide study of QTLs related to flowering time evaluated potential candidate genes underlying those QTLs (Kamal et al. 2019). Specific alleles on chromosomes 1, 4, 14, 17, and 18 were found to be associated with early flower time using a population derived from a breeding line (GF.GA-47-42) via 'Villard Blanc' cross. In another study, single nucleotide polymorphisms (SNPs) on chromosome 16 were associated with berry development (e.g., time from flowering to maturity) (Guo et al. 2019). It is well-known that a major QTL on linkage group 18 affects berry weight and seedlessness (Costantini et al. 2008; Doligez et al. 2002; Mejía et al. 2007, 2011). Additional stable QTLs have been identified on linkage groups 1, 7, 8, 11, 17, and 19, depending on the study and cross used (Doligez et al. 2013; Guo et al. 2019; Houel et al. 2015). The complexity of these traits clearly demonstrate their quantitative nature and may require additional robust markers to effectively capture and select for the desired allelic variation in breeding programs.

Historically, cluster size has been less-studied compared with other traits, partly because it is primarily of importance for table and not wine grapes. Recently, several studies have evaluated mapping populations and diverse panels for heritability of cluster size. For cluster size, studies have identified QTLs on chromosomes 14, 15, and 16 (Richter et al. 2019a, 2019b). The QTL on 16 was also found in a separate study, along with a novel QTL on chromosome 9; however, these QTLs were not consistent between years (Underhill et al. 2020). One study using a genome-wide association approach identified a novel locus on chromosome 13 for cluster weight but was unable to detect a significant QTL on chromosomes 9, 14, 15, or 16 (Laucou et al. 2018). Similar to berry shape and size, this lack of consistent QTLs is likely attributable to the variability among germplasm within and among grape species.

In many of the previously mentioned studies, markers were not tested in materials outside the initial mapping population in which they were identified, and transferability was not evaluated. This lack of transferability testing, coupled with the highly quantitative aspect of fruit quality traits, has been a limitation for implementing marker-assisted selection of these traits. As more breeders use interspecific crosses for incorporating traits of interest, it is imperative to test the transferability of markers across an array of materials to determine their usefulness. This study aimed to identify QTLs associated with fruit quality traits useful for breeding high-quality grape cultivars and test the transferability of newly and previously identified markers using a diverse set of grape cultivars.

## Materials and Methods

**Plant materials and DNA extractions.** Approximately 215 mature vines of a previously described mapping population [C81-227 (*V. cinerea*) × Y315-43-04 (*V. vinifera*)] with fruit trait variability (Cadle-Davidson et al. 2016) located at the San Joaquin Valley Agricultural Sciences Center (Parlier, CA, USA) were evaluated (Table 1, Fig. 1). Each vine represented a genetically unique $F_1$ individual from the *Vitis* interspecific hybrid cross (*V. cinerea* × *V. vinifera*). Plants were spaced ∼1 m apart with 2-m row spacing on a T trellis system. Vines were fertilized, watered, and treated for management of powdery mildew as needed. In Apr 2018, one 2-cm piece of young leaf tissue from each vine was placed into each well of a 96-well collection plate. Two stainless steel beads were placed in each well, and filled plates were frozen at −80 °C. Once frozen, tissue was pulverized with an automated tissue grinder (SPEX Sample Prep, Metuchen, NJ, USA). DNA was extracted using Qiagen Plant DNeasy kits according to the kit directions (Qiagen, Hilden, Germany) modified with the addition of 2% polyvinylpyrrolidone 40 in the extraction buffer.

We conducted *rh*AmpSeq sequencing as described by (Yin et al. 2021; Zou et al. 2020). To identify haplotype variants, *rh*AmpSeq marker data were analyzed using a custom Perl script (Analyze_amplicon.pl), which was further converted to a variant-

Received for publication 18 Jul 2023. Accepted for publication 28 Nov 2023.
Published online 23 Jan 2024.
We thank Dr. Lu Yin, Sofia Maldonado, Marcos Alvarez, Cameron Saunders, and Karen Vasquez for technical assistance. Sequencing was performed by the Biotechnology Resource Center (BRC) Genomics Facility (RRID:SCR_021727) at the Cornell Institute of Biotechnology (http://www.biotech.cornell.edu/brc/genomics-facility). Mention of a concept, idea, trade name, or commercial product in this publication is solely for the purpose of providing specific information and does not imply recommendation or endorsement by the US Department of Agriculture (USDA). The USDA is an equal opportunity employer.
This work was funded, in part, by the US Department of Agriculture Agricultural Research Service (USDA-ARS) (project 8080-21000-032-00-D and 2034-21220-007-00D), as well as the USDA-National Institute of Food and Agriculture (NIFA) Specialty Crop Research Initiative (award no. 2017-51181-26829).
On behalf of all authors, the corresponding author states that there is no conflict of interest. The authors have no relevant financial or nonfinancial interests to disclose.
All authors contributed to manuscript preparation, study conception, and design. Material preparation and data collection were performed by Amy Tabb, Jason Londo, Sonet van Zyl, Bernard Prins, Alanna Burhans, Jeff DeLong, Hui-Ching Yang, Matt Clark, and Rachel Naegele. Data analyses were performed by Laise de Sousa Moreira, Amy Tabb, Jeff DeLong, Alanna Burhans, Hui-Ching Yang, Cheng Zou, Avinash Karn, Qi Sun, and Rachel Naegele. The first draft of the manuscript was written by Rachel Naegele. All authors commented on previous versions of the manuscript. All authors read and approved the final manuscript.
The datasets generated during and/or analyzed during the current study are provided in supplemental materials or are available from the corresponding author on reasonable request.
R.N. is the corresponding author. E-mail: Rachel.naegele@usda.gov.

Table 1. Grapevine traits evaluated for an interspecific hybrid population (11-3527) from 2016 to 2019 at the US Department of Agriculture-Agricultural Research Service San Joaquin Valley Agricultural Sciences Center (Parlier, CA, USA).

| Trait | Short name | Description | Method | Units measured | Years when traits were evaluated |
|---|---|---|---|---|---|
| Flowering time | FT | 50% of cluster had reached anthesis | Visual assessment | Days, GDD[i] | 2016, 2017, 2018, 2019 |
| Veraison time | VT | Time when berry transitions from growth to softening and ripening | Visual assessment | Days, GDD | 2016, 2017, 2018, 2019 |
| Full color time | FC | Time when 90% of cluster has color (red and black cultivars only) | Visual assessment | Day, GDD | 2016, 2017, 2018, 2019 |
| Berry color | BC | Berry skin color | Visual assessment | Green, red or black | 2016, 2017, 2018 |
| Berry weight | BW | Berry weight | Scale | Grams | 2016, 2017, 2018 |
| Berry number | BNo | Total number of berries in a cluster | Visual assessment | Number | 2016 |
| Estimated berry number | EBNo | Total berry weight/average berry weight based on a random 10-berry sample | Scale | Grams | 2017, 2018, 2019 |
| Berry size-width | BSW | Minor axis of the grape berry equivalent to width | Scanner | Millimeter | 2016, 2017, 2018 |
| Berry size-length | BSL | Major axis of the grape berry equivalent to length | Scanner | Millimeter | 2016, 2017, 2018 |
| Berry size- area | BSA | Total area of the berry calculated from the major axis * minor axis | Scanner | Millimeter | 2016, 2017, 2018 |
| Berry shape | BS | Berry roundness or eccentricity | Scanner | No units | 2016, 2017, 2018 |
| Soluble solids | SS | Brix or sugar content | Brix meter | Degrees | 2016 |
| Cluster weight | CWt | Total weight of cluster not including rachis | Scale | Grams | 2017, 2018 |
| Cluster length | CL | Maximum length of cluster (berry space only) | Computer vision | Millimeter | 2018, 2019 |
| Cluster width | CW | Maximum width of cluster (berry space only) | Computer vision | Millimeter | 2018, 2019 |

[i] Growing degrees days accumulation base 10 °C, 1 Jan.

calling format file using the haplotype_to_VCF.pl Perl script (Karn 2021). The *rh*AmpSeq markers targeted 250 bp regions evenly distributed across the genome. Because there could be multiple polymorphisms (SNPs and indels) in each region, each marker represented up to four alleles in the $F_1$ population studied.

As reported by Zou et al. (2020), multidimensional scaling and Mendelian error detection were performed as quality controls to identify vines with genotyping errors caused by self-pollination, pollen contamination, or mislabeling. An identical × state kinship matrix computed using TASSEL 5 (Bradbury et al. 2007) was used to conduct the multidimensional scaling analysis, which was further visualized using the R *ggplot2* package (Wickham 2011).

Fig. 1. Representative clusters demonstrating population variability in cluster size, color, and shape for individuals from an interspecific *Vitis* hybrid population (11-3527).

Similarly, the Mendelian error detection analysis was conducted using *mendelian* plugin in *bcftools* (Danecek et al. 2011, 2021).

**Genetic map construction.** A genetic map was constructed with Lep-MAP3 version 0.2 (Rastas 2017) using the variant-calling format files and the pedigree information of each vine in the population. The following Lep-MAP3 modules and steps were used to construct the genetic maps: (1) *ParentCall2* module of Lep-MAP3 was used to call parental genotypes; (2) *Filtering2* module was used to filter distorted markers based on a chi-squared test and monomorphism; (3) the *SeparateChromosomes2* module was used to split the marker into linkage groups; and (4) the *OrderMarkers2* module was used to order the markers within each linkage group using 20 iterations per group, computing parental (sex-specific) and sex-averaged genetic distances. The marker order of the genetic maps was evaluated for consistency, genome organization, and structural variation by correlating markers with their physical coordinates on the *V. vinifera* PN40024 reference genome (version 12X.v2) (Canaguier et al. 2017). Finally, the phased output data from the OrderMarkers2 step were converted into four-way phased genotype data using the *map2gneotpes.awk* script (Rastas 2017). A sex-averaged genetic map consisting of 849 markers across 19 chromosomes was used to detect all QTLs.

**Trait evaluations.** A phenotypic evaluation was conducted from 2016 to 2019. After berry set, each vine was thinned to 10 or fewer clusters depending on the total number of clusters available per vine. Approximately five grape clusters from each

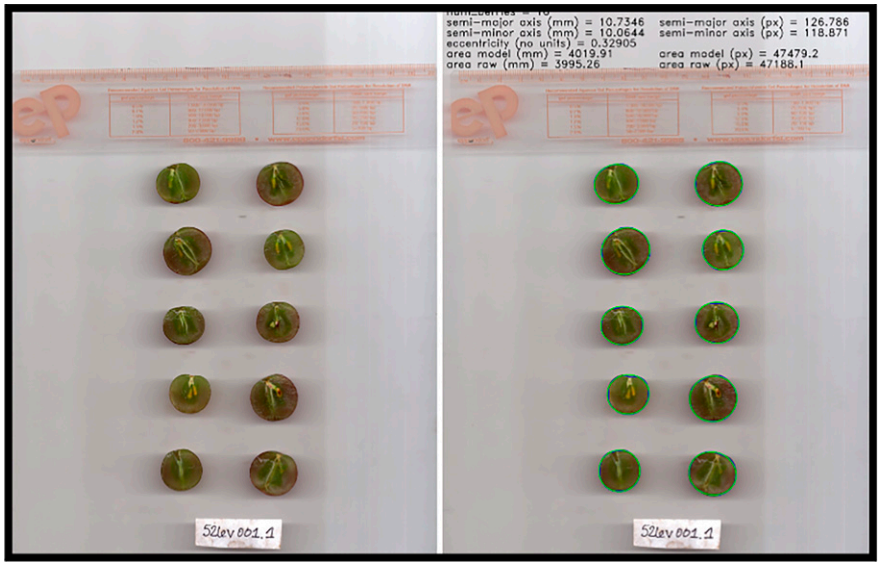


Fig. 2. Raw *Vitis* sp. berry image (left) and processed berry image with calculated metrics (right).

genotype, represented as a unique vine, were evaluated. Flowering time for each cluster was measured as time to >50% anthesis. Veraison time was measured as the date of the first color (red berry clusters) or berry softening (green berry clusters only). Full color was described as the time when 90% of the berries exhibited color (red berry clusters only). Time for each phenological phase was calculated as the calendar day of the year (CDY) and as growing degree day (GDD) accumulation (base 10 °C; 1 Jan) based on weather data provided by the California irrigation management information system station at University of California Kearney in Parlier, CA, USA. For all other evaluations, clusters were harvested at full color and evaluated in the laboratory. Berry shape and size were determined using two-dimensional images of 10 representative berries from each cluster collected using a flatbed scanner (Epson V2 perfection; Epson America, Carson, CA, USA) with a ruler included for size reference. Two-dimensional images of grape clusters were obtained using a Nikon D3300 camera (Nikon, Melville, NY, USA) and an ArUco pattern for sizing reference (2018 and 2019). The number of berries per cluster was counted by hand (2017) or estimated based on the average berry weight divided by the total weight of the berries. The average berry weight (2016, 2017, 2018, 2019) was calculated by measuring the bulk weight of 10 representative berries and dividing by 10. Cluster weight (2017, 2018, 2019) was measured by weighing all of the berries from a cluster and did not include the rachis weight. Not all vines produced five clusters that reached maturity; therefore, not all individuals were represented for each trait each year. Data were collected from 150 to 180 individuals, depending on the trait and year.

**Image-based analyses.** A computer vision algorithm was developed using Mask R-CNN (He et al. 2017), as implemented by Abdulla (2017), to segment individual berries from the background and find the parameters for the elliptical model using the algorithm of Halõr and Flusser (1998). The method was developed using a training set of 67 images and a validation set of 13 images. These images were drawn from the full dataset. Training set labels of berry and nonberry pixels were generated using a classical computer vision algorithm.

For cluster image analyses, the background for the clusters was prepared with ArUco markers (Garrido-Jurado et al. 2014) printed on aluminum and placed underneath the clusters, with paper between the cluster and the aluminum (Fig. 2). A camera as scanner (Tabb et al. 2022) was used to calibrate the camera for each image and allow for measurements to be computed from the image in millimeters. For pixel-to-millimeter conversion for the camera as scanner, the number was set at 3. The image was segmented into a grape cluster (white) and nongrape cluster (black) regions using intensity information from the ArUco tags (Tabb et al. 2022). To account for any slight variation in the camera angle, the image was warped such that 3 pixels were equivalent to 1 mm and preliminarily segmentated. Only regions where the area was larger than 500 pixels were considered to eliminate spurious detections. To only account for berry regions in the image (not stem/rachis), the largest stem or stem joint regions were estimated to be no more than 12 mm; consequently, the image was eroded and dilated by that amount to only capture the berry regions in the image. The axis-aligned bounding box of the remaining white regions was computed to provide the length and width of the cluster (Fig. 3).

**Statistics and quantitative trait loci mapping.** A mean value for each trait averaged across all clusters collected for each genotype was calculated each year. Based on the methodology described by Miller et al. (2022), trait means were corrected across years by calculating the year effect for the years associated with each trait and correcting an individual's overall mean best linear unbiased prediction. Before performing the QTL analysis, the normality of trait data was assessed using visual inspection of histograms. QTL analyses were performed using the R/QTL package (version 3.6.1) under the interval mapping standards with scanone function, the "Kosambi" map function, "imp'' algorithm method, and four-way cross-type (Broman and Sen 2009; R Core Team 2019). The minimum logarithm of odds score required for QTL detection was determined by the genome-wide logarithm of odds significance threshold ($\alpha = 0.05$) based on 1000 permutations. The contribution of a QTL on a phenotypic trait variance was also estimated using the fitQTL function.

Fig. 3. Raw cluster image (left) and processed cluster image with bounding box (right) in *Vitis* sp.

**Marker validation.** A diverse panel of commercially available grape cultivars was selected from field- or greenhouse-grown plants available at the San Joaquin Valley Agricultural Sciences Center (Table 2). Two-centimeter leaves were collected from each vine and returned to the laboratory for lyophilization and DNA extractions. Lyophilized tissue was disrupted using the Qiagen Tissuelyser, and DNA was extracted using the Qiagen Plant DNA kit of the Qiacube HT. Kompetitive allele specific polymerase chain reaction (PCR) (KASP) markers were developed for newly identified QTLs, explaining more than 10% of the variability when possible (Supplemental Table 1). In brief, the marker design targeted 100 bp on either side of the associated SNP, and sequences were downloaded based on the PN40024 reference genome (The French-Italian Public Consortium for Grapevine Genome Characterization 2007). Primers (Sigma-Aldrich, St. Louis, MO, USA) were developed using IDT PrimerQuest Tool (Integrated DNA Technologies, Coralville, IA, USA), with the causal SNP being the 3′ end of the forward primer (Patterson et al. 2017; Yin et al. 2022). A binding site for FAM (GAAGGTGACCAAGTTCATGCT) was attached to the 5′ end of the forward primer for the causal SNP, and a binding site for HEX (GAAGGTCGGAGTCAACGGATT) was attached to the 5′ end of the forward primer for the alternate SNP (Patterson et al. 2017). The KASP assay was performed according to the manufacturer's guide (LGC Genomics, Hoddeson, UK) and He et al. (2014). In brief, an assay mix was first created with 10 mM Tris-HCl (pH 8.3) and the following three primers: 100 μM of the FAM-labeled forward primer (final 12 μM), the HEX-labeled forward primer (final 12 μM), and the common reverse primer (final 30 μM). Next, the reaction mix for a 96-well plate was prepared by combining 432 μL of 2X KASP Master Mix (LGC Genomics) and 11.88 μL of the assay mix. For each DNA sample, the KASP reaction was performed in a total volume of 8 μL, with 4 μL of the reaction mix and 4 μL of DNA (final, 20–30 ng). A no template control was included in each experiment. KASP thermal cycling was conducted using Bio-Rad CFX Opus (Bio-Rad Laboratories, Hercules, CA, USA) with the following programs: one cycle of 94 °C for 15 min; 10 cycles of 94 °C for 20 s; 61 to 55 °C for 1 min with 0.6 °C drop per cycle; 23 °C for 30 s; 26 cycles of 94 °C for 20 s; 55 °C for 1 min; and a final of plate read at 37 °C for 1 min. After the initial run, the allelic discrimination was examined using CFX Maestro software (Bio-Rad). If the distinction among genotype groupings had not been formed, then recycling of the assay plate was performed with three cycles of 94 °C for 20 s, 57 °C for 1 min, and a final of plate read at 37 °C for 1 min. The recycling step was repeated until the clusters were formed.

Table 2. Grape cultivar diversity panel representing wine, table, juice, and American grape (*Vitis*) species used for evaluating marker transferability.

| Grape cultivar | Use type |
|---|---|
| Autumn King | Table grape |
| Autumn Royal | Table grape |
| Cabernet Sauvignon | Wine grape |
| Cayuga White | Wine grape (H[i]) |
| Chardonnay | Wine grape |
| Crimson seedless | Table grape |
| Dovine | Raisin grape |
| Fiesta | Raisin grape |
| Flame seedless | Table grape |
| Horizon | Juice grape (H) |
| Niagara | Juice grape (H) |
| Pixie | Microvine |
| Princess | Table grape |
| Red Globe | Table grape |
| Sauvignon Blanc | Wine grape |
| Scarlet Royal | Table grape |
| Selma Pete | Raisin grape |
| Solbrio | Table grape |
| Summer Royal | Table grape |
| Sunpreme | Raisin grape |
| Tampa | Wine grape (H) |
| Thompson seedless | Raisin grape |
| Valley Pearl | Table grape |
| Zinfandel | Wine grape |

[i] A *Vitis* interspecific hybrid.

**Previously published marker evaluation.** Previously published fruit quality-associated simple sequence repeat (SSR)-based markers were tested against the 11-32527 population and compared with phenotypic data of phenology and berry traits (Supplemental Table 2). For each primer set, previously published PCR annealing conditions were used using the Promega GoTaq Mastermix (Promega Corporation Madison, WI, USA) with 1 μL of DNA (20 ng·μL$^{-1}$). For those primer sets that did not result in a product with the published PCR annealing conditions, a gradient PCR was used to improve resolution. PCR products were visualized on a 4% agarose gel run at 60 V for 1 h. For bands that did not show a visible separation using agarose, the template was run again using M-13 tailed primers and visualized using gel electrophoresis on an Applied Biosystems 3730xl 96-capillary DNA Analyzer. Fifteen primer pairs of the 11-32527 population as well as 24 previously established commercial cultivars were evaluated to detect potential PCR product band variability relative to the QTL position associated with each marker set. A three-primer method (Schuelke 2000) was used for marker examination of the 11-32527 population. The forward primer for each fruit quality marker had an 18-bp M13 tag (5′- TGTAA AACGACGGCCAGT-3′) attached to the 5′ end. The reverse primer contained a "pigtail" sequence (5′- GTTTCTT-3′) on the 5′ end, which was added to promote adenylation and reduce stuttering (Brownstein et al. 1996). The third primer consisted of the

M13 tag labeled with a 6-FAM fluorescent dye (Invitrogen Inc., Waltham, MA, USA) on the 5′ end.

PCR was performed for 25 μL reactions and contained 12.5 μL of 2X GoTaq Clear Master Mix (Promega Corp.), 0.75 μL of 10 μM forward primer, 2.0 μL of 10 μM reverse primer, 1.25 μL of 10 μM 5′6FAM-labeled M13 tag primer (Invitrogen Inc.), and 7.0 μL of ultrapure and 1.5 μL of ~30.0 ng·μL$^{-1}$ DNA template. Reaction conditions were 95 °C for 2 min, followed by 32 cycles of denaturation at 95 °C for 30 s, annealing at a temperature varying between 53 and 60 °C, (specific to the optimal temperature based on the primer design) for 30 s, extension at 72 °C for 30 s, and a final extension at 72 °C for 5 min. One microlite of a 1:10 dilution of PCR product was added to 0.3 μL of GeneScan 500 LIZ-labeled size standard and 9.7 μL of Hi-Di formamide (Thermo Fisher Scientific, Waltham, MA, USA). Amplicons were denatured by incubation at 95 °C for 5 min and immediately placed on ice. A fragment analysis was conducted using an Applied Biosystems 3730xl 96-capillary DNA Analyzer. Geneious v.11.0.3 (Kearse et al. 2012) was used to determine allele sizes based on electropherograms. Standard gel electrophoresis was conducted using a 2% (weight/volume) agarose gel (Cambrex BioScience Rockland, Inc., East Rutherford, NJ, USA) for 2.5 h at 95 V (4.75 V/cm) using a 100-bp size standard (New England Biolabs Inc., Ipswich, MA, USA) for some of the marker sets to confirm amplification of PCR products within the expected size range.

Marker presence/absence or size (bp) variations were evaluated against cluster images. Clusters of each vine were imaged using an SLR camera (Nikon D3300) and placed onto a white background with a yardstick included for size reference. Previously published primers were also tested against the same commercial cultivar panel used for marker validation, representing wine, table, and raisin grape cultivars with known cluster and phenology characteristics. Relative size categories vary among the use types of table, wine, and raisin grapes, and listed sizes were adjusted so that they were based on table grapes.

**Structural comparisons of chromosome 18.** For chromosome 18, the 30.00- to 34.56850-Mb region of the PN40024 reference genome (repeats were removed) was used for structural comparisons among sequenced grape genomes as previously described (Canaguier et al. 2017; The French-Italian Public Consortium for Grapevine Genome Characterization 2007). The target region was aligned with the PN40024 reference genome using minimap2 with the preset parameter for genome alignment (asm10) (2.17) (Li 2018). Similar regions for representatives of *V. rupestris*, *V. vinifera*, *V. cinerea*, *V. labrusca,* and three interspecific hybrids were also aligned with the reference genome using the preset parameter for genome alignment as previously described (Li 2018).

## Results

**Phenotypic evaluations.** All of the traits evaluated during this study showed large variation across individuals and years. Not all individuals were represented in each year because disease pressure and fruitfulness varied among the vines. Flowering time in the population ranged from 411 to 635 GDD in 2016, 290 to 609 GDD in 2017, and 485 to 643 GDD in 2018 (Table 3). Similarly, using CDY, flowering time varied depending on the year (111 to 136 d, 100 to 140, and 128 to 144 d in 2016, 2017, and 2018, respectively). The veraison time varied from 903 to 1627 GDD, 1028 to 2616, and 988 to 2171, and 1061 to 2088 in 2016, 2017, 2018, and 2019, respectively. Similar to flowering time, veraison time varied greatly depending on the year from 157 to 204, 171 to 262, 171 to 237, and 175 to 237 d in 2016, 2017, 2018, and 2019, respectively, when using CDY as well. Time to full color (FC) in the population ranged from 1123 to 1931 GDD, 1164 to 2616, 1153 to 2212, and 1184 to 2534 in 2016, 2017, 2018, and 2019, respectively (Table 3). In CDY, this ranged from 175 to 221 d, 178 to 262, 181 to 241, and 184 to 267 in 2016, 2017, 2018, and 2019, respectively (Supplemental Table 3).

Berry weight ranged from 1.61 to 6.79 g, 0.69 to 8.88 g, 0.92 to 11.90, and 0.76 to 7.73 g in 2016, 2017, 2018, and 2019, respectively, in the population. Cluster weight (CW) ranged from 17.93 to 975.8 g, 32.6 to 1006.8 g, and 64 to 1041.10 g. Berry number per cluster ranged from 18.6 to 414.0 (2017 only). Estimated berry number in 2018 and 2019 ranged from 11 to 241 and 23 to 247, respectively. Berry shape or eccentricity ranged from 0.25 to 0.56, 0.23 to 0.625, and 0.25 to 0.59 in 2016, 2017, and 2018, respectively, indicating most berries in the population

Table 3. Population averages for evaluated phenology and berry traits evaluated in a *Vitis* sp. interspecific hybrid population (11-3527) from 2016 to 2019.

| | 2016 | | 2017 | | 2018 | | 2019 | |
|---|---|---|---|---|---|---|---|---|
| Trait | Mean | *SD* | Mean | *SD* | Mean | *SD* | Mean | *SD* |
| Flowering time (GDD)[i] | 474.33 | 84.1 | 501.87 | 36.69 | 521.06 | 31.33 | | |
| Veraison time (GDD) | 1284.92 | 151.52 | 1501.65 | 264.19 | 1387.55 | 212.69 | | |
| Full color (GDD) | 1514.12 | 157.30 | 1841.26 | 261.76 | 1748.02 | 259.35 | | |
| Berry weight (g)[ii] | 3.87 | 1.17 | 4.25 | 1.9 | 5.09 | 2.09 | 3.63 | 1.4 |
| Berry size — area ($mm^2$)[iii] | 3397.89 | 770.33 | 3944.83 | 880.46 | 4358.25 | 1059.95 | | |
| Berry number | | | 76.42 | 41.60 | | | | |
| Estimated berry number | | | | | 81.02 | 43.16 | 96.71 | 44.42 |
| Berry shape | 0.36 | 0.08 | 0.36 | 0.08 | 0.36 | 0.07 | | |
| Cluster weight (g) | | | 328.25 | 189.99 | 413.09 | 251.58 | 328.71 | 157.4 |
| Cluster length (mm)[iv] | | | | | 242.20 | 66.02 | 251.24 | 45.79 |
| Cluster weight (g) | | | | | 153.24 | 39.87 | 150.15 | 30.21 |

[i] Growing degree days.
[ii] Grams.
[iii] Area in square millimeters.
[iv] Millimeters.

were round and not ellipsoid (Table 3). Berry size (area in $mm^2$) ranged from 1964 to 5289, 1972 to 6139, and 1371 to 6657 $mm^2$ in 2016, 2017, and 2018, respectively.

**QTL analyses.** Based on best linear unbiased predictions, QTLs for berry traits were primarily associated with chromosome 18. Major and minor axes of the berry size and berry area identified major QTLs in a similar (within 5 Mb) region at the end of chromosome 18, explaining ∼21% to 24% of the variability. A minor QTL on chromosome 9, explaining almost 13% of the variability, was also associated with the minor axis of berry shape (Table 4). When individual years were evaluated, an additional QTL on chromosome 8 associated with berry shape (eccentricity), explaining 13% to 28% of the variability, was identified in 2016 and 2018 (Supplemental Table 4). No QTLs were detected when years were combined for berry shape. Berry number was only counted in 2017, and a QTL on chromosome 14 at 39 cM (marker 14_21821143) explained 25% of the variability observed. For estimated berry number, QTLs were detected on chromosome 14 (similar location to the QTL identified with direct counting in 2017) and chromosome 18 (18_14846541). The QTL on chromosome 14 explained the majority of the variation observed (∼29%), whereas the QTL on chromosome 18 was more minor (∼14%). Berry weight was controlled by QTLs located on chromosomes 7, 9, and 18, explaining ∼12% to 28% of the variation observed.

For cluster traits, a QTL for CW was identified on chromosome 14, explaining 27% of the variability (Table 4). A possible additional QTL that had overlapping confidence intervals with the first was identified when years were evaluated separately. QTLs for cluster length (CL) and CW (data from only one year) were identified on chromosomes 7, 10, and 14, explaining almost 8% to 18% of the variability. No QTLs for the CL:CW ratio were detected.

For berry development, QTLs were detected on chromosomes 18 (11%), 17 and 18 (13%–19%), and 12 and 17 (14%–20%) for flowering time, veraison time, and FC, respectively. The QTLs on chromosome 17 for veraison time (17_6623514) and FC (17_5893163) had overlapping intervals but showed distinct peaks. Similarly, for the QTL on chromosome 18, there was an overlap in the intervals between the QTL for flowering time (18_1360028) and the QTL for veraison time (18_9598522), but distinct peaks were evident.

**Previous SSRs.** Not all SSRs successfully amplified in all individuals in the commercial or 11-3527 test panel. It should be noted that these markers are not considered predictive of a trait, but they were shown to be "associated" with the respective trait. No consistent variability in size or presence/absence was observed between previously published markers for flowering, veraison or ripening time, berry number, fruit maturation, or seed weight using the 11-3527 population (Supplemental Table 5). Markers VMC2D9 and VVMD25 had low or no allelic variability in the population. Low band size variability was observed among individuals for all of the markers tested, and presence/absence was more frequently observed. When compared with the commercial cultivar panel, fragment size (bp) variability was detected for markers VMC1E11, VVMD27, VMC1B11, VMC6C10, VMC7F2, VMC2H4, and VMC2C10. These markers, associated with fruit development (flowering, veraison, or ripening) time or berry characteristics (berry number, seed presence, total berries) showed little ability to predict differences among commercial grape cultivars evaluated (Supplemental Table 6). However, the marker associated with seed weight (VMC7F2) was able to differentiate seedless cultivars with a high degree of consistency (13/13) and misidentified only three of the 10 seeded cultivars as "seedless".

**Marker transferability.** A set of KASP markers based on 13 QTLs identified during this study were tested against the commercial test panel for their ability to predict the respective trait of interest. None of the KASP markers showed a high level of association between the presence of a SNP and the trait of interest across all use types or genetic backgrounds (Supplemental Table 7). Some markers, including those associated with berry weight (7_19355564), FC (17_1513957 and 17_5893163), berry number (14_21821143), and flowering time (18_13860028), had little to no variability among the commercial test panel genotypes. When evaluated within a use type (wine, table, raisin or hybrid grape), potential associations were observed with KASP

Table 4. Quantitative trait loci associated with berry and phenology traits based on best linear unbiased estimate predictions using the expectation-maximization algorithm for genetic mapping in the 11-3527 (*Vitis cinerea* × *V. vinifera*) population.

| Trait | Chr[i] | Pos[ii] | Marker | LOD[iii] | Variability (%) | *P* value |
|---|---|---|---|---|---|---|
| Berry size length | 18 | 81 | 18_34381037 | 9.66 | 24.27 | <0.001 |
| Berry size width | 9 | 22 | 9_6990766 | 4.69 | 12.64 | 0.021 |
| | 18 | 84 | 18_31132460 | 8.16 | 20.93 | <0.001 |
| Berry shape area | 18 | 76 | 18_34381037 | 9.36 | 23.63 | <0.001 |
| Flowering time | 18 | 43 | 18_13860028 | 4.23 | 11.08 | 0.05 |
| Veraison time | 17 | 37 | 17_6623514 | 7.62 | 19.34 | <0.001 |
| | 18 | 34 | 18_9598522 | 5.12 | 13.16 | 0.029 |
| Time to full color | 12 | 28 | 12_8142405 | 4.92 | 14.11 | 0.016 |
| | 17 | 31 | 17_5893163 | 7.27 | 20.13 | 0.001 |
| Berry weight | 7 | 70 | 7_19355564 | 4.40 | 11.56 | 0.041 |
| | 9 | 22 | 9_6990766 | 5.34 | 13.86 | 0.007 |
| | 18 | 80 | 18_334381037 | 11.85 | 28.09 | <0.001 |
| Estimated berry number | 14 | 61 | 14_26877597 | 12.10 | 28.81 | <0.001 |
| | 18 | 50 | 18_14846541 | 5.20 | 13.60 | <0.001 |
| Cluster weight | 14 | 62 | 14_27729833 | 11.47 | 27.69 | <0.001 |

[i] Chromosome.
[ii] Position.
[iii] Logarithm of odds.

markers, but sample sizes were low. Cluster height (marker 7_8252505) had limited predictability for wine grape, with a heterozygous state of allele 1 and allele 2 (A1/A2) being associated with longer clusters and allele 2 (A2) associated with shorter clusters. No large wine grape clusters were included in the panel. Marker 17_6745403 showed a potential association with time to full color of table grapes, but it showed no predictability for time to full color for wine, raisin, or hybrid grapes. For table grapes, A1 for marker 17_6745403 was associated with a reduced time to full color, whereas allele 3 (A3) or the heterozygous state of A1/A3 were associated with longer time to full color (Supplemental Table 7). For marker 17_6623514, A3 was associated with late time to veraison and A2 was associated with early veraison time of raisin grapes, but not of table, wine, or hybrids. For marker 8_96364, A1 was more frequently associated with an oval shape (6/7) compared with A2, which was more frequently associated with a round (8/10) berry shape of table, wine, and hybrid grapes. *Vitis* hybrids, *V. labrusca* juice grape ('Niagara'), and 'Tampa' (*Vitis aestivalus* × 'Niagara') had the highest number of "no call" datapoints across all markers with nine and six, respectively (Supplemental Table 7).

**Chromosome variability.** Structural alignment of the end of chromosome 18 associated with multiple identified QTLs, a region associated with variability in berry size, shape, and weight, was performed for 'Cabernet Sauvignon', 'Concord' (*V. labrusca,* PI 588077), 'Jaeger 70' (*V. aestivalus* × *V. lincecumii* × *V. rupestris*, PI 588234), Cham ('Chambourcin', PI 588075), Rupestris1 (*V. rupestris*, PI 588160), *V. cinerea* (PI 588154), Doan. (*Vitis* ×*doaniana*, PI 588149), 'Flame Seedless' (table grape), and 'Sultanina' (syn. 'Thompson Seedless') (table/raisin grape) (Fig. 4). The two table grape cultivars, Flame Seedless and Sultanina, had the highest percentages (>75%) of similarity across this region compared with wine grape cultivars (<52%) (Cabernet Sauvignon and Jaeger), juice grapes (60%) (Concord), and wild species (<50%) (*V. cinerea* and *V. rupestris*) (Table 5).

## Discussion

Flowering time is major step in the long process of berry development and ripening and is an important consideration when adopting a new cultivar. Times to different points of grape phenology (flowering, veraison, and full ripening/full color) have been evaluated across multiple crosses and breeding programs over the years. QTLs associated with time to flowering from budbreak have been found on chromosomes 7 and 14 (Duchene et al. 2012) and 1, 10, 11, 14, and 17 (Fechter et al. 2014). Many of these QTLs had a minor effect on the trait (7% to 14%) and showed little overlap with the other study. More recently, a study that examined genes and alleles associated with early flowering time found positive candidates near QTL regions on chromosomes 1, 4, 14, 17, and 18, suggesting that many, if not all, of these regions may be useful for selecting early flowering time of grape depending on the genetic background (Kamal et al. 2019). We identified a single QTL on chromosome 18, explaining ~11% of the variability observed. This region was similar to a significant gene associated with early flowering time observed by Kamal et al. (2019). In a meta-QTL analysis, veraison time was most affected by QTLs and genes on chromosomes 14, 16, and 18, similar to the results of Duchene et al. (2012), identifying QTLs associated with time from flowering to veraison on 16 and 18 (Delfino et al. 2019). Additional QTLs associated with veraison time were located on chromosomes 1, 2, and 13, but these contributed less (Delfino et al. 2019). In our study, QTLs were identified on chromosomes 1 (one year only), 17, and 18. Although a QTL on chromosomes 1 and 18 have been identified in several studies, a QTL on chromosome 17 has been found in only two other populations using primarily *V. vinifera* crosses (Costantini et al. 2008; Duchene et al. 2012; Fechter et al. 2014; Grzeskowiak et al. 2013; Richter et al. 2019a; Zyprian et al. 2016).

Berry quality traits are an integral part of cultivar development for table and wine grapes. Many QTLs for berry and fruit

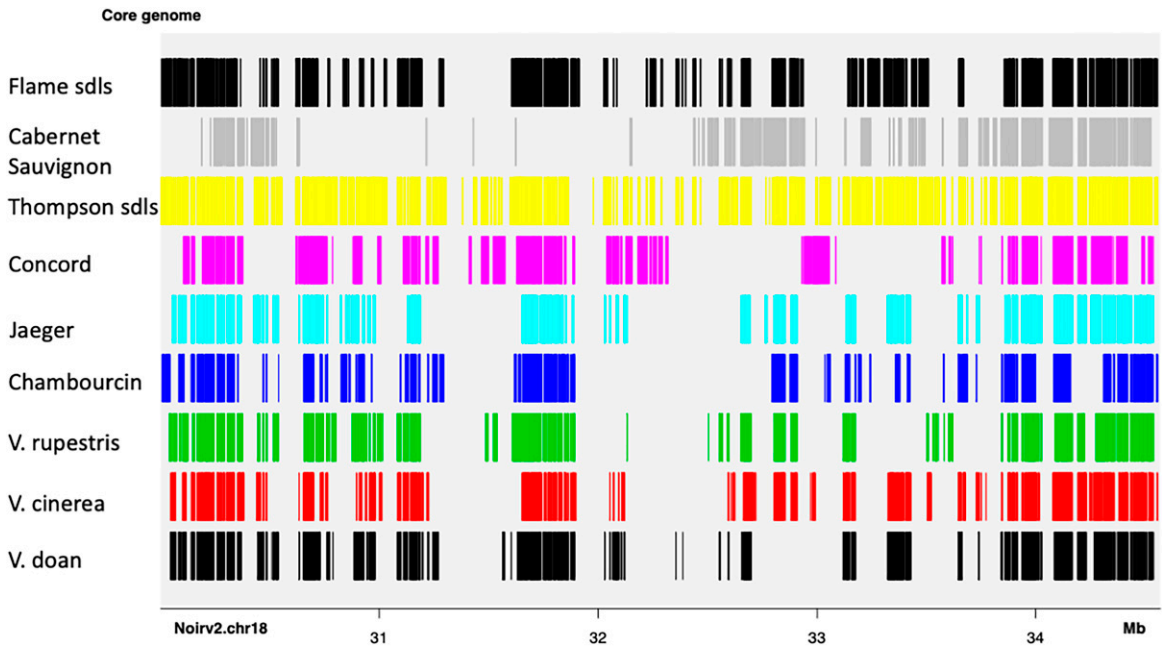


Fig. 4. Structural alignment of the end of chromosome 18 from *Vitis vinifera* (Flame sdls, Cabernet Sauvignon, Thompson sdls), *V. rupestris*, *V. cinerea*, *V. labrusca* (Concord), and three interspecific hybrids (Chamburcin, Jaeger, V.doan) to the 30- to 34-Mb end of chromosome 18 on the PN40024 genome.

Table 5. Alignment percentages for the end of chromosome 18 to the grape (*Vitis*) reference genome (PN40024[i]) among sequenced grapes.

| Grape ID | Form | Species | Aligned length (bp) | Total length (bp) | Proportion aligned (%) |
|---|---|---|---|---|---|
| Rup1 | Wild | *V. rupestris* | 1165776 | 2348675 | 49.6 |
| Flame seedless | Table | *V. vinifera* | 1816575 | 2348675 | 77.3 |
| Sultanina | Table | *V. vinifera* | 2337184 | 2348675 | 99.5 |
| Cine | Wild | *V. cinerea* | 1217428 | 2348675 | 51.8 |
| Jaeger 70 | Interspecific hybrid | *V. aestivalis* × *V. rupestris* | 1179395 | 2348675 | 50.2 |
| Concord | Juice | *V. labrusca* | 1430874 | 2348675 | 60.9 |
| Doan | Interspecific hybrid | *V. acerifolia* × *V. mustangensis* | 1233892 | 2348675 | 53.0 |
| Chambourcin | Interspecific hybrid | *Vitis* sp. cv. Chambourcin | 1055354 | 2348675 | 44.9 |
| Cabernet Sauvignon | Wine | *V. vinifera* | 1220492 | 2348675 | 52.1 |

[i] The French-Italian Public Consortium for Grapevine Genome Characterization (2007).

quality traits have been identified for grape from *V. vinifera*, *V. labrusca*, and other *Vitis* sp., and often have variable effects based on the genetic background. In a *V. labrusca* × *V. vinifera* interspecific hybrid cross, a QTL on chromosome 11 was identified as a major player in berry weight, whereas in *V. vinifera* crosses, chromosome 18 appears to play a major role in berry weight (Ban et al. 2016). A more recent study using a panel of 179 grape genotypes identified the same locus on chromosomes 18 for berry weight, as well as additional loci on chromosomes 19 and 17 (Guo et al. 2019). Similar work by Underhill et al. (2020) (a complex interspecific *Vitis* hybrid population) and Ban et al. (2016) also identified chromosome 11 as having a major stable QTL contributing to berry weight. In our study, a locus on chromosome 18 was the major driver of berry weight in the 11-3527 (*V. cinerea* × *V. vinifera*) population. However, additional QTLs were also detected with minor effects on chromosomes 7 and 9 when using data combined across years. These QTLs may be population- or *V. cinerea*-specific and less useful for breeding new *V. vinifera* cultivars. A QTL located on a similar region of chromosome 7 was detected during one additional study using a microvine that had a *V. vinifera* background (Houel et al. 2015).

Wine and juice grapes, as well as most other *Vitis* species, typically have round, spherical berries with little variability in overall shape. In contrast, table grapes have more diversity in shape, and some programs have historically selected for specific shapes (Wycislo et al. 2008). More recently, breeding for berry shapes has gained increased interest as specialty table grapes have been released with unique attributes, including extremely elongated elliptical forms. Berry shape, typically called the berry shape index, was explored in a table grape population, and a novel significant QTL on chromosome 8 was identified (Wang et al. 2020). During our work, berry shape was described as eccentricity or how well a berry fit roundness, and a single QTL on chromosome 8 was also identified. Depending on the year, this QTL explained almost 30% of the variability observed.

Although some of the regions associated with specific berry traits identified in this study explained >15% of the variability observed, more work is necessary to refine QTL regions and identify underlying genes. From a breeding perspective, KASP markers developed from SNPs identified during this study showed little ability to predict traits of interest across grape use types and will mostly be useful within a use type. This variability may be attributable, in part, to genetic and structural differences among pedigrees, and also differences in terms like "early" and "late" that can be relative within a use type. For example, wine grapes tend to be harvested at a later date than table grapes to maximize soluble solids levels, and an "early" harvested wine grape may coincide with the same time point as a "mid" or "late" season table grape.

Cluster traits, such as weight and length, in addition to shape, are also important for grapes. QTLs for cluster weight have been found on chromosomes 4, 9, and 16 using a wine grape cross with a diverse genetic background (Underhill et al. 2020), on chromosome 13 using a diverse panel of grape genotypes (Laucou et al. 2018), and on 14, 15 and 16 (Richter et al. 2019b). Our study also located a QTL on chromosome 14 associated with cluster weight during all three years evaluated, controlling 15% to 24% of the variability, indicating that it is likely to be stable. QTLs associated with cluster length have been found in several studies, but they also varied among years and populations. In a wine grape cross, QTLs for cluster length were found on chromosomes 9, 16, and 17, depending on the year (Underhill et al. 2020), and 10, 12, 17, and 18 (Richter et al. 2019a, 2019b). Studies have also examined SNPs in specific genes associated with aspects of cluster length, i.e., rachis length, located on chromosomes 5, 7, 10, 12, and 18 (Tello et al. 2016, 2020). During our study, cluster length or height, was associated with QTLs on chromosomes 7 and 10, suggesting that both regions may be targets for transferable markers. However, no QTL for cluster length was associated with chromosome 18 in our population.

Many of the differences in QTLs and marker transferability are likely to be the result of the different species, use types, and parents used in these studies. Grapes are highly heterozygous with both genetic and structural variations and have more than 80 species described; of these, at least seven (*V. vinifera, V. labrusca, V. cinerea, V. amurensis, V. riparia, V. arizonica, V. champinii*) have been regularly used for breeding (Krivanek et al. 2005; Migicovsky et al. 2016). Selective sweeps during domestication have been documented based on grape use type (raisin, table, wine, and juice) and may play a role in the limited marker transferability observed to date (Kui et al. 2020; Migicovksy et al. 2016). One study found that chromosomes 12, 14, and 15 had the highest SNP densities overall compared with the reference genome; however, when examined by commodity type, strong selection signals were found on chromosomes 18 for table grapes and 11 for wine grapes (Kui et al. 2020). QTL studies have been consistent with the idea of a selective sweep on chromosome 18 for berry-related traits, including size and veraison time. A major QTL with potentially pleiotropic effects for berry-related traits has been routinely identified on chromosome 18 across populations and studies, consistent with our results. We further compared this region across several grape species and cultivars and revealed high variability in structure among

and between types (wine vs. juice vs. table) and species. Table grape cultivars had the highest structure similarity for this region (>75%) compared with other cultivated grapes and species, consistent with a selective sweep for table grapes.

Similar to many plant systems, QTL studies of grape are important for identifying loci associated with traits of interest for both breeding and genetic studies. However, markers developed often are not transferrable to other crosses or genetic backgrounds because of high heterozygosity and the diversity of materials used in breeding. In this study, we identified QTLs (novel and previously known) associated with fruit quality and development characteristics using an interspecific hybrid population. We also evaluated the ability of existing SSR-based markers to accurately predict berry traits across a panel of commercial cultivars. A region at the end of chromosome 18 was associated with multiple traits, including flowering time, berry weight, number, shape, and size, and was further evaluated for structural differences across multiple grape species and cultivars. High variability was observed among non-*V. vinifera* species and wine grapes (*V. vinifera*), whereas table grape cultivars (*V. vinifera*) showed low variability, consistent with previous reports of a selection sweep on chromosome 18.

## References Cited


Abdulla W. 2017. Mask R-CNN for object detection and instance segmentation on Keras and TensorFlow. Github. https://github.com/matterport/Mask_RCNN.

Ban Y, Mitani N, Sato A, Kono A, Hayashi T. 2016. Genetic dissection of quantitative trait loci for berry traits in interspecific hybrid grape (*Vitis labruscana* × *Vitis vinifera*). Euphytica. 211:295–310. https://doi.org/10.1007/s10681-016-1737-8.

Bradbury PJ, Zhang Z, Kroon DE, Casstevens TM, Ramdoss Y, Buckler ES. 2007. TASSEL: Software for association mapping of complex traits in diverse samples. Bioinformatics. 23:2633–2635. https://doi.org/10.1093/bioinformatics/btm308.

Broman KW, Sen ŚA. 2009. Guide to QTL mapping with R/QTL in statistics for biology and health. Springer, New York, NY, USA.

Brownstein MJ, Carpten JD, Smith RJ. 1996. Modulation of non-templated nucleotide addition by TaqDNA polymerase: primer modifications that facilitate genotyping. Biotechniques. 20:1004–1006. https://doi.org/10.2144/96206st01.

Burger P, Vermeulen A, Halleen F, Koopman T, van Heerden CJ, Prins R. 2014. Table grape breeding at the ARC INFRUITEC-NIETVOORBIJ, South Africa; It's impact on the SA industry and latest developments. Acta Hortic. 1046:245–249. https://doi.org/10.17660/ActaHortic.2014.1046.31.

Cadle-Davidson L, Gadoury D, Fresnedo-Ramirez J, Yang S, Barba P, Sun Q, Demmings EM, Seem R, Schaub M, Nowogrodzki A, Kasinathan H, Ledbetter C, Reisch BI. 2016. Lessons from a phenotyping center revealed by the genome-guided mapping of powdery mildew resistance loci. Phytopathology. 106:1159–1169. https://doi.org/10.1094/PHYTO-02-16-0080-FI.

Canaguier A, Grimplet J, Di Gaspero G, Scalabrin S, Duchêne E, Choisne N, Mohellibi N, Guichard C, Rombauts S, Le Clainche I, Bérard A, Chauveau A, Bounon R, Rustenholz C, Morgante M, Le Paslier MC, Brunel D, Adam-Blondon AF. 2017. A new version of the grapevine reference genome assembly (12x.v2) and of its annotation (Vcost.v3). Genom Data. 14:56–62. https://doi.org/10.1016/j.gdata.2017.09.002.

Costantini L, Battilana J, Lamaj F, Fanizza G, Grando MS. 2008. Berry and phenology-related traits in grapevine (*Vitis vinifera* L.): From Quantitative Trait Loci to underlying genes. BMC Plant Biol. 8:38. https://doi.org/10.1186/1471-2229-8-38.

Danecek P, Auton A, Abecasis G, Albers CA, Banks E, DePristo MA, Handsaker RE, Lunter G, Marth GT, Sherry ST, McVean G, Durbin R. 2011. The variant call format and VCFtools. Bioinformatics. 27:2156–2158. https://doi.org/10.1093/bioinformatics/btr330.

Danecek P, Bonfield JK, Liddle J, Marshall J, Ohan V, Pollard MO, Whitwham A, Keane T, McCarthy SA, Davies RM, Li H. 2021. Twelve years of SAMtools and BCFtools. GigaScience. 10:giab008. https://doi.org/10.1093/gigascience/giab008.

Delfino P, Zenoni S, Imanifard Z, Battista Tornielli G, Bellin D. 2019. Selection of candidate genes controlling veraison time in grapevine through integration of meta-QTL and transcriptomic data. BMC Genomics. 20:739. https://doi.org/10.1186/s12864-019-6124-0.

Doligez A, Bertrand Y, Farnos M, Grolier M, Romieu C, Esnault F, Dias S, Berger G, Francois P, Pons T, Ortigosa P, Roux C, Houel C, Laucou V, Bacilieri R, Peros JP, This P. 2013. New stable QTLs for berry weight do not colocalize with QTLs for seed traits in cultivated grapevine (*Vitis vinifera* L.). BMC Plant Biol. 13:217. https://doi.org/10.1186/1471-2229-13-217.

Doligez A, Bouquet A, Danglot Y, Lahogue F, Riaz S, Meredith C, Edwards K, This P. 2002. Genetic mapping of grapevine (*Vitis vinifera* L.) applied to the detection of QTLs for seedlessness and berry weight. Theor Appl Genet. 105:780–795. https://doi.org/10.1007/s00122-002-0951-z.

Duchene E, Butterlin G, Dumas V, Merdinoglu D. 2012. Towards the adaptation of grapevine varieties to climate change: QTLs and candidate genes for developmental stages. Theor Appl Genet. 124:623–635. https://doi.org/10.1007/s00122-011-1734-1.

Fechter I, Hausmann L, Zyprian E, Daum M, Holtgräwe D, Weisshaar B, Topfer R. 2014. QTL analysis of flowering time and ripening traits suggests an impact of a genomic region on linkage group 1 in *Vitis*. Theor Appl Genet. 127:1857–1872.

Fidelibus M, El-kereamy A, Haviland D, Hembree K, Zhuang G, Steward T, Sumner DA. 2018. Sample costs to establish and produce table grapes. University of California Agricultural and Natural Resources Cooperative Extension Agricultural Issues Center UC Davis Department of Agricultural and Resource Economics.

Garrido-Jurado S, Muñoz-Salinas R, Madrid-Cuevas FJ, Marín-Jiménez MJ. 2014. Automatic generation and detection of highly reliable fiducial markers under occlusion. Pattern Recognit. 47:2280–2292. https://doi.org/10.1016/j.patcog.2014.01.005.

Grzeskowiak L, Costantini L, Lorenzi S, Stella Grando M. 2013. Candidate loci for phenology and fruitfulness contributing to the phenotypic variability observed in grapevine. Theor Appl Genet. 126:2763–2776. https://doi.org/10.1007/s00122-013-2170-1.

Guo DL, Zhao HL, Li Q, Zhang GH, Jiang JF, Liu CH, Yu YH. 2019. Genome-wide association study of berry-related traits in grape [*Vitis vinifera* L.] based on genotyping-by-sequencing markers. Hortic Res. 6:1–13. https://doi.org/10.1038/s41438-018-0089-z.

Halõr R, Flusser J. 1998. Numerically stable direct least squares fitting of ellipses. Proc. 6th International Conference in Central Europe on Computer Graphics and Visualization. WSCG. 98:125–132.

He K, Gkioxari G, Dollár P, Girshick R. 2017. Mask r-cnn. Proceedings of the IEEE International Conference on Computer Vision. 2961–2969.

He C, Holme J, Anthony J. 2014. SNP genotyping: The KASP assay, p 75–86. In: Fleury D, Whitford R (eds). Crop breeding, methods in molecular biology. Springer, New York, NY, USA.

Houel C, Chatbanyong R, Doligez A, Rienth M, Foria S, Luchaire N, Roux C, Adiveze A, Lopez G, Farnos M, Pellegrino A, This P, Romieu C, Torregrosa L. 2015. Identification of stable QTLs for vegetative and reproductive traits in the microvine (*Vitis vinifera* L.) using the 18 K Infinium chip. BMC Plant Biol. 15:205. https://doi.org/10.1186/s12870-015-0588-0.

Kamal N, Ochßner I, Scwandner A, Viehöver P, Hausmann L, Töpfer R, Weisshaar B, Holtgräwe D. 2019. Characterization of genes and alleles involved in the control of flowering time in grapevine. PLoS One. 14:e0214703. https://doi.org/10.1371/journal.pone.0214703.

Karn A. 2021. Analyze amplicon. https://github.com/avinashkarn/analyze_amplicon. [accessed 1 Dec 2021].

Kearse M, Moir R, Wilson A, Wilson A, Stones-Havas S, Cheung M, Sturrock S, Buxton S, Cooper A, Markowitz S, Duran C, Thierer T, Ashton B, Meintjes P, Drummond A. 2012. Geneious Basic: an integrated and extendable desktop software platform for the organization and analysis of sequence data. Bioinformatics. 28:1647–1649. https://doi.org/10.1093/bioinformatics/bts199.

Krivanek AF, Stevenson JF, Walker MA. 2005. Development and comparison of symptom indices for quantifying grapevine resistance to Pierce's Disease. Phytopathology. 95:36–43. https://doi.org/10.1094/phyto-95-0036.

Kui L, Tang M, Duan S, Wang S, Dong X. 2020. Identification of selective sweeps in the domesticated table and wine grape (*Vitis vinifera* L.). Front Plant Sci. https://doi.org/10.3389/fpls.2020.00572.

Laucou V, Launay A, Bacilieri R, Lacombe T, Adam-Blondon AF, Bérard A, Chauveau A, de Andrés MT, Hausmann L, Ibáñez J, Le Paslier MC, Maghradze D, Martinez-Zapater JM, Maul E, Ponnaiah M, Töpfer R, Péros JP, Boursiquot JM. 2018. Extended diversity analysis of cultivated grapevine *Vitis vinifera* with 10K genome-wide SNPs. PLoS One. 13:e0192540. https://doi.org/10.1371/journal.pone.0192540.

Li H. 2018. Minimap2: Pairwise alignment for nucleotide sequences. Bioinformatics. 24:3094–3100. https://doi.org/10.1093/bioinformatics/bty191.

Mejía N, Gebauer M, Muñoz L, Hewstone N, Muñoz C, Hinrichsen P. 2007. Identification of QTLs for seedlessness, berry size, and ripening date in a seedless x seedless table grape progeny. Am J Enol Viticult. 58:499–507. https://doi.org/10.5344/ajev.2007.58.4.499.

Mejía N, Soto B, Guerrero M, Casanueva X, Houel C, Miccono ML, Ramos R, Le Cunff L, Boursiquot JM, Hinrichsen P, Adam-Blondon AF. 2011. Molecular, genetic and transcriptional evidence for a role of *VvAGL11* in stenospermocarpic seedlessness in grapevine. BMC Plant Biol. 11:57. https://doi.org/10.1186/1471-2229-11-57.

Migicovsky Z, Sawler J, Money D, Eibach R, Miller AJ, Luby JJ, Jamieson AR, Velasco D, von Kintzel S, Warner J, Wuhrer W, Brown PJ, Myles S. 2016. Genomic ancestry estimation quantifies use of wild species in grape breeding. BMC Genomics. 17:478. https://doi.org/10.1186/s12864-016-2834-8.

Miller BA, Kostick SA, Luby JJ. 2022. Large-effect QTLs for titratable acidity and soluble solids content validated in 'Honeycrisp'-derived apple germplasm. Agronomy. 12:1703. https://doi.org/10.3390/agronomy12071703.

Mira de Orduna R. 2010. Climate change associated effects on grape and wine quality and production. Food Res Int. 43:1844–1855. https://doi.org/10.1016/j.foodres.2010.05.001.

Myles S, Boyko AR, Owens CL, Brown PJ, Grassi F, Aradhya K, Prins B, Reynolds A, Chia JM, Ware D, Bustamante CD, Buckler ES. 2010. Genetic structure and domestication history of the grape. Proc Natl Acad Sci USA. 108:3530–3535. https://doi.org/10.1073/pnas.1009363108.

Patterson EL, Fleming MB, Kessler KC, Nissen SJ, Gaines TA. 2017. A KASP genotyping method to identify norther watermilfoil, Eurasian watermilfoil, and their interspecific hybrids. Front Plant Sci. 8:00752. https://doi.org/10.3389/fpls.2017.00752.

R Core Team. 2019. R: A language and environment for statistical computing. R Foundation for Statistical computing, Vienna, Austria. https://www.R-project.org/.

Rastas P. 2017. Lep-MAP3: Robust linkage mapping even for low-coverage whole genome sequencing data. Bioinformatics. 33:3726–3732. https://doi.org/10.1093/bioinformatics/btx494.

Richter R, Gabriel D, Rist F, Töpfer R, Zyprian E. 2019a. Identification of co-located QTLs and genomic regions affecting grapevine cluster architecture. Theor App. Genet. 132:1159–1177. https://doi.org/10.1007/s00122-018-3269-1.

Richter R, Rossmann S, Gabriel D, Töpfer R, Theres K, Zyprian E. 2019b. Differential expression of transcription factor- and further growth-related genes correlates with contrasting cluster architecture in *Vitis vinifera* 'Pinot Noir' and *Vitis* spp. genotypes. Theor Appl Genet. 133:3249–3272. https://doi.org/10.1007/s00122-020-03667-0.

Santos JÁ, Fraga H, Malheiro A, Moutinho-Pereira J, Dinis LT, Correia C, Moriondo M, Leolini L, Dibari C, Costafreda-Aumedes S, Kartschall T, Menz C, Molitor D, Junk J, Beyer M, Schultz HR. 2020. A review of the potential climate change impacts and adaptation options for European viticulture. Appl. Sci 10:3092. https://doi.org/10.3390/app10093092.

Schuelke M. 2000. An economic method for the fluorescent labeling of PCR fragments. Nat Biotechnol. 18:233–234. https://doi.org/10.1038/72708.

Tabb A, Holguín GA, Naegele RP. 2022. Using cameras for precise measurement of two-dimensional plant features: CASS, p 87–94. In: Lorence A, Jimenez KM (eds). High-throughput plant phenotyping: Methods and protocols. Humana, New York, NY, USA. https://doi.org/10.1007/978-1-0716-2537-8.

Tello J, Torres-Perez R, Grimplet J, Ibanez J. 2016. Association analysis of grapevine bunch traits using a comprehensive approach. Theor Appl Genet. 129:227–242. https://doi.org/10.1007/s00122-015-2623-9.

Tello J, Torres-Perez R, Flutre T, Grimplet J, Ibanez J. 2020. *VviUCC1* nucleotide diversity, linkage disequilibrium and association with rachis architecture traits in grapevine. Genes (Basel). 11:598. https://doi.org/10.3390/genes11060598.

Terral JF, Tabard E, Bouby L, Ivorra S, Pastor T, Figueiral I, Picq S, Chevance JB, Jung C, Fabre L, Compan M, Bacilieri R, Lacombe T, This P. 2010. Evolution and history of grapevine (*Vitis vinifera*) under domestication: New morphometric perspectives to understand seed domestication syndrome and reveal origins of ancient European cultivars. Ann Bot. 105:443–455. https://doi.org/10.1093/aob/mcp298.

The French-Italian Public Consortium for Grapevine Genome Characterization. 2007. The grapevine genome sequence suggests ancestral hexaploidization in major angiosperm phyla. Nature. 449:463–467. https://doi.org/10.1038/nature06148.

Underhill A, Hirsch C, Clark M. 2020. Image-based phenotyping identifies quantitative trait loci for cluster compactness in grape. J Am Soc Hortic Sci. 145:363–373. https://doi.org/10.21273/JASHS04932-20.

van Leeuwen C, Darriet P. 2016. The impact of climate change on viticulture and wine quality. J Wine Econ. 11:150–167. https://doi.org/10.1017/jwe.2015.21.

Wang H, Yan A, Sun L, Zhang G, Wang X, Ren J, Xu H. 2020. Novel stable QTLs identification for berry quality traits based on high-density genetic linkage map construction in table grape. BMC Plant Biol. 20:411. https://doi.org/10.1186/s12870-020-02630-x.

Wickham H. 2011. Ggplot2. WIREs Comp Stat. 3:180–185.

Wycislo AP, Clark JR, Karcher DE. 2008. Fruit shape analysis of *Vitis* using digital photography. HortScience. 43:677–680. https://doi.org/10.21273/HORTSCI.43.3.677.

Yamada M, Sato A. 2016. Advances in table grape breeding in Japan. Breed Sci. 66:34–45. https://doi.org/10.1270/jsbbs.66.34.

Yin L, Karn A, Cadle-Davidson L, Zou C, Underhill A, Atkins P, Treiber E, Voytas D, Clark M. 2021. Fine mapping of leaf trichome density revealed a 747-kb region on chromosome 1 in cold-hardy hybrid wine grape populations. Front Plant Sci. 12:587640. https://doi.org/10.3389/fpls.2021.587640.

Yin L, Karn A, Cadle-Davidson L, Zou C, Londo J, Sun Q, Clark MD. 2022. Candidate resistance genes to foliar phylloxera identified at Rdv3 of hybrid grape. Hort Res. 9:uhac027. https://doi.org/10.1093/hr/uhac027.

Zou C, Karn A, Reisch B, Nguyen A, Sun Y, Bao Y, Campbell MS, Church D, Williams S, Xu X, Ledbetter CA, Patel S, Fennell A, Glaubitz JC, Clark M, Ware D, Londo JP, Sun Q, Cadle-Davidson L. 2020. Haplotyping the *Vitis* collinear core genome with rhAmpSeq improves marker transferability in a diverse genus. Nature Comm. 11:413. https://doi.org/10.1038/s41467-019-14280-1.

Zyprian E, Ochßner I, Schwander F, Simon S, Hausmann L, Bonow-Rex M, Moreno-Sanz S, Grando M, Wiedemann-Merdinoglu S, Merdinoglu D, Elbach R, Töpfer R. 2016. Quantitative trait loci affecting pathogen resistance and ripening of grapevines. Mol Genet Genomics. 291:1573–1594. https://doi.org/10.1007/s00438-016-1200-5.